

An Inverse Heat Transfer Model of Thermal Degradation Within Multifunctional Tensioned Cable Structures

P.G. Moore, H.N. Jones, III, and S.G. Lambrakos

(Submitted June 2, 2004)

A method for the analysis of heat transfer within a multifunctional tensioned cable structure, resulting from external heating by the impingement of a hot gas, is presented. This method, which is based on inverse analysis, uses a conveniently applicable parametric model representation. The problem of failure prediction due to the thermal degradation of the various components within complex cable structures can be difficult due to the lack of information concerning both the anisotropic thermal properties that are typical of these composite structures, and the heat transfer between components internally. The method of analysis presented here provides a means of overcoming these difficulties and conveniently analyzing the performance of multifunctional tensioned cable structural elements that are subject to external heating. Prototype simulations of heat transfer within a complex cable structure using the inverse parametric model representation are presented.

Keywords anisotropic properties, cable structures, heat transfer, inverse analysis

1. Introduction

Failure due to thermal degradation within a multifunctional tensioned cable structure can be difficult to predict because, in general, both the anisotropic thermal properties and the internal heat-transfer paths that are inherent with these structures are not well defined. This is because cable structures are normally used for multiple purposes. For example, the cable generally must sustain high tensile stresses, which require a structural element, and may incorporate both power and control lines. The structural component must also have sufficient stiffness at peak loads to limit the strains induced in the insulated metal wires and fiber optic signal strands. Given these general characteristics of multifunctional cable structures, it is to be expected that a physical model representation for predicting failure resulting from the exposure to a specific heating environment should present a problem requiring significant levels of effort in terms of both mathematical analysis and computer simulation. This level of effort may not be appropriate for the practical analysis of performance and failure predictions of complex cable structures. Methods of inverse analysis, however, provide a means for the quantitative prediction of performance characteristics, while at the same time minimizing the inclusion of inconvenient levels of mathematical complexity (Ref 1). These methods are especially convenient for the analysis of thermal response using thermocouple measurements (Ref 2, 3). In this work, a relatively simple and conveniently applicable model representation of heat transfer within complex cable structures is presented, based on inverse engi-

neering, for the analysis of the structural response due to thermal degradation. This model is applied to a prototype analysis of a cable structure consisting of graphite/phthalonitrile composite strands. This prototype analysis serves two purposes: first, it serves as an example of model calibration, or parameter adjustment, according to experimental measurements of the temperature field via thermocouples that are distributed at various positions on the cable structure; and second, it is used as an example of simulations for predicting structural failure due to thermal breakdown resulting from the exposure of a given linear structure of a composite nature to a specific external heat source.

2. Parametric Model Representation

For unsteady heat deposition within a cable structure of a finite cross section, a consistent parametric representation of the time-dependent temperature field is:

$$T(x, y, z, t) = \sum_{k=1}^{N_k} \sum_{n=1}^{N_t} T_k(x_k, y_k, z_k, n\Delta t) \quad (\text{Eq 1})$$

where

$$T_k(x_k, y_k, z_k, n\Delta t) = T_A + \frac{C(x_k, y_k, z_k)}{\sqrt{n\Delta t}} \exp\left[-\frac{(x-x_k)^2}{4\kappa_1(n\Delta t)}\right] \\ \times \left\{ 1 + 2 \sum_{m=1}^{\infty} \exp\left[-\frac{\kappa_2 m^2 \pi^2 (n\Delta t)}{a^2}\right] \cos\left[\frac{m\pi y}{a}\right] \cos\left[\frac{m\pi y_k}{a}\right] \right. \\ \left. \times \left\{ 1 + 2 \sum_{m=1}^{\infty} \exp\left[-\frac{\kappa_3 m^2 \pi^2 (n\Delta t)}{l^2}\right] \cos\left[\frac{m\pi z}{l}\right] \cos\left[\frac{m\pi z_k}{l}\right] \right\} \right\} \quad (\text{Eq 2})$$

In these equations, T_A is the ambient temperature of the cable structure and the time $t = N_t \Delta t$ ($N_t = 1, 2, 3, \dots$) is expressed

P.G. Moore, H.N. Jones, III, and S.G. Lambrakos, Materials Science and Technology Division, Code 6320, Naval Research Laboratory Washington, D.C. 20375-5000. Contact e-mail: lambrakos@anvil.nrl.navy.mil.

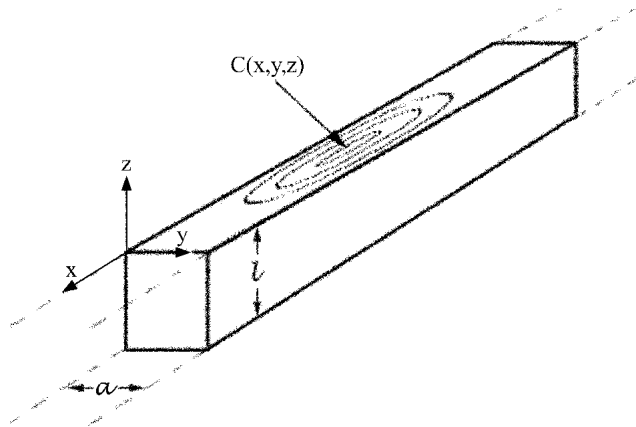


Fig. 1 Schematic representation of the model multifunctional cable structure

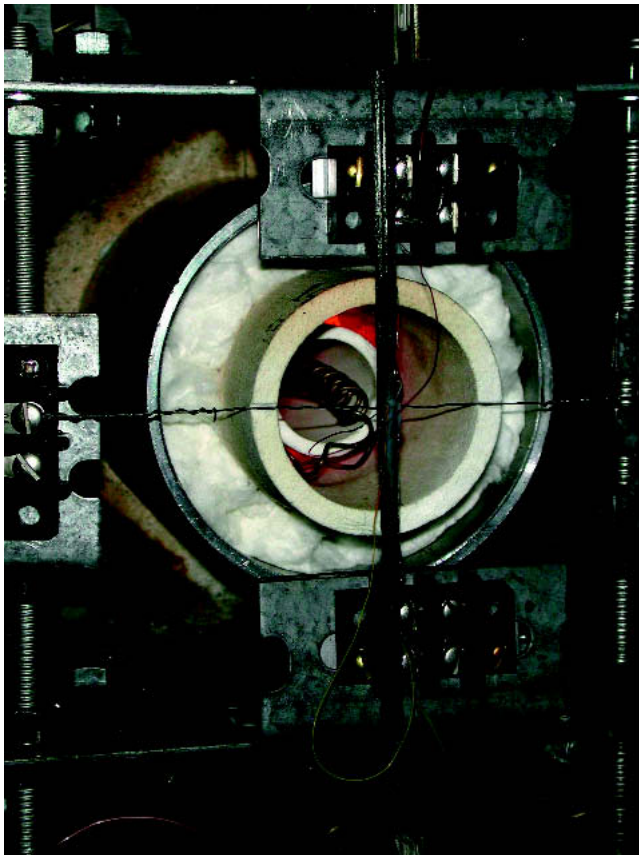


Fig. 2 Overall view of the experimental arrangement used for heating the prototype cable structure

as N_t multiples of discrete time steps, Δt . The coefficients $C(x_k, y_k, z_k)$, which specify the spatial distribution of discrete surface heat elements, and the diffusivities κ_1, κ_2 , and κ_3 are adjustable parameters of the inverse model defined by Eq 1 and 2. The quantities a and l are the lengths of the sides of the rectangular cross section of the wire structure (Fig. 1). In general, the wire structure is characterized by an anisotropic thermal diffusivity such that the “through-thickness” diffusivities (i.e., κ_2 and κ_3)

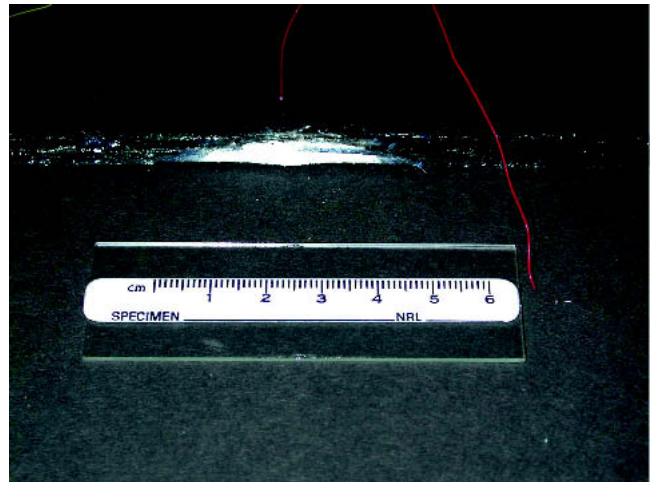


Fig. 3 C fiber prototype cable structure after testing showing a silica coating resulting from decomposition of the silicone rubber. This silica coating insulated the cable structure from further heating, even though the hot air temperature was increased.

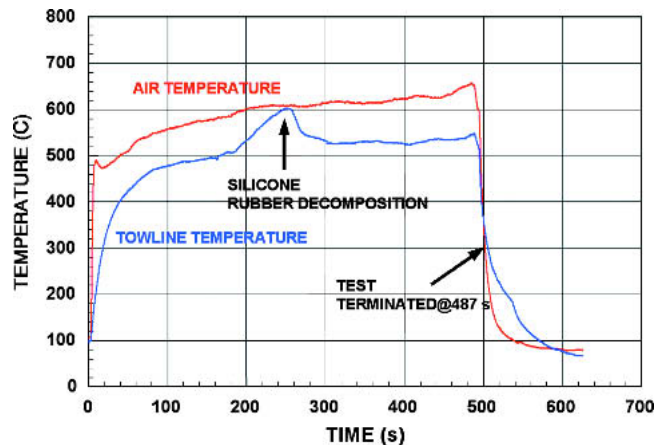


Fig. 4 Temperature history of a graphite fiber composite strand prototype cable structure. The internal temperature reached 600 °C (1112 °F), after which point the silicone rubber decomposed to form a silica coating that insulated the cable.

are significantly less than the “in-plane” diffusivity κ_1 . The spatial coordinates (x_k, y_k, z_k) and (x, y, z) are the discrete locations of the heat elements on the surface of the model wire structure and positions within the wire structure at which the calculated temperature is defined, respectively (Fig. 1). The solution to the heat conduction equation given by Eq 2 represents a modification of that given in Ref 4.

3. Prototype Analysis

The cable structure considered for the present analysis was a silicone rubber-impregnated coated assembly with carbon (C) fiber strands having a rectangular cross section, $a = 3.175$ mm (0.125 in.) and $l = 6.350$ mm (0.25 in.). Surface heating of this prototype cable structure was achieved using an electric hot air source, the maximum air temperature of which was 600 °C.

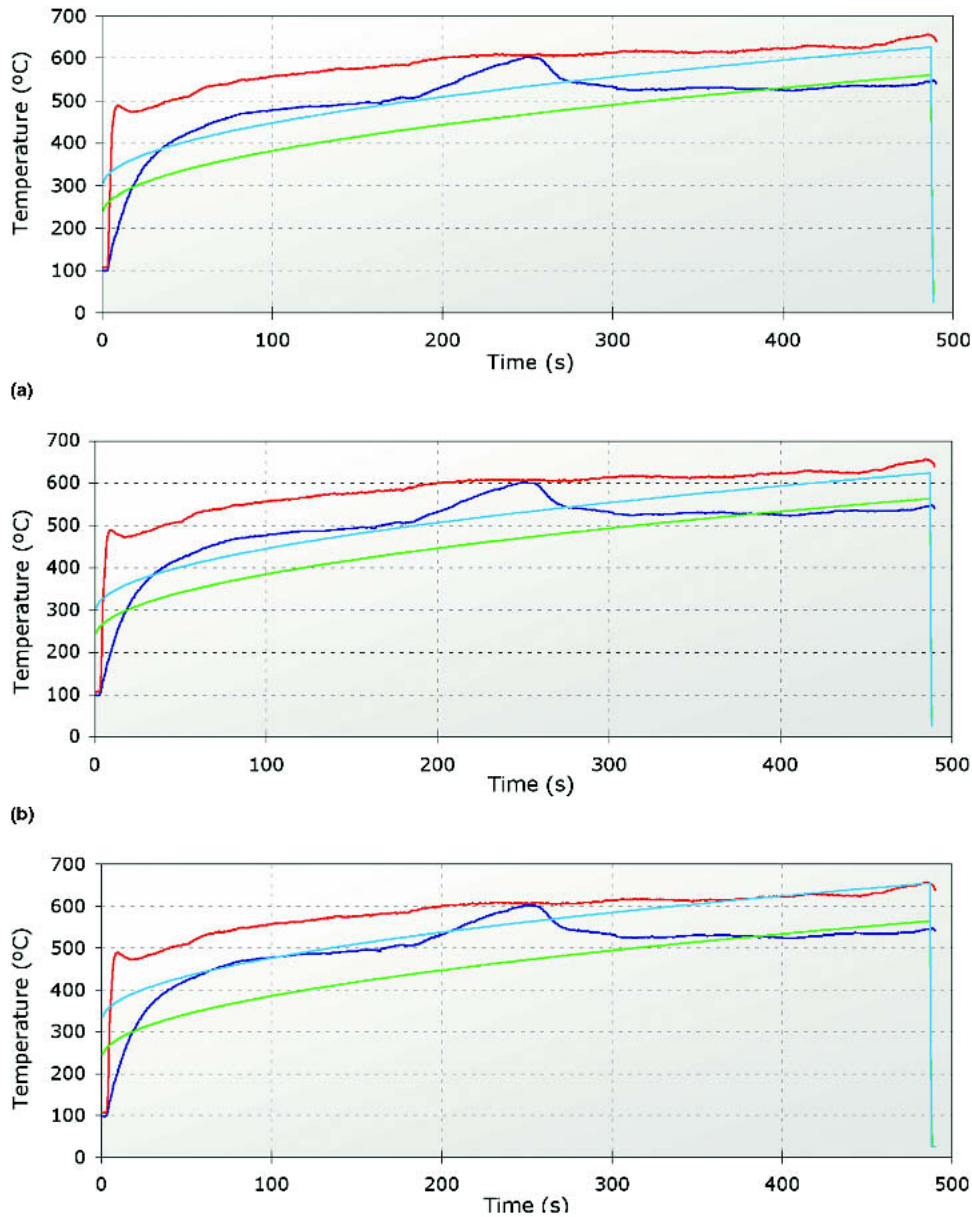


Fig. 5 Comparison of the calculated and experimentally measured temperature histories for three different modes of thermal conduction. (a) $\kappa_1 = 7.7 \times 10^{-4} \text{ m}^2/\text{s}$, $\kappa_2 = \kappa_1$, $\kappa_3 = \kappa_1$; $\kappa_1 = 3.0 \times 10^{-3} \text{ m}^2/\text{s}$, (b) $\kappa_2 = 0.27\kappa_1$, $\kappa_3 = \kappa_2$; and (c) $\kappa_1 = 3.7 \times 10^{-3} \text{ m}^2/\text{s}$, $\kappa_2 = 0.0176\kappa_1$, $\kappa_3 = \kappa_2$. Bottom and top “coarse” curves are for experimentally measured temperatures at the center and on the surface, respectively. Bottom and top “smooth” curves are for simulated temperatures at the center and on the surface, respectively.

Shown in Fig. 2 and 3 are the experimental arrangements for heating and the prototype cable structure, respectively. The heating pattern after an experiment, shown in Fig. 3, which appears white, is correlated with the formation of a silica coating resulting from the decomposition of the silicone rubber matrix of the cable structure. This pattern was adopted for assigning the spatial distribution of surface heat elements (i.e., the values of coefficients C and a set of positions (x_k, y_k, z_k) defined in Eq 2). For the purpose of this prototype analysis, two thermocouple measurements were made during the heating period. One thermocouple was attached within the center of the cable structure, below the point of maximum heating, while the

other was attached on the surface of the structure at the point of maximum heating from the hot air source. Shown in Fig. 4 are temperature histories corresponding to thermocouple measurements at these two positions, on and within the graphite-fiber prototype cable structure. Also shown in Fig. 4 is a signature corresponding to the exothermic reaction associated with silicone rubber decomposition.

In the case of the prototype cable structure considered here, there is not any time of failure, which correlates with actual mechanical breakage or cracking. Further, the time period prior to the decomposition of the silicone rubber coating is not assumed as the time prior to failure. For the purposes of this

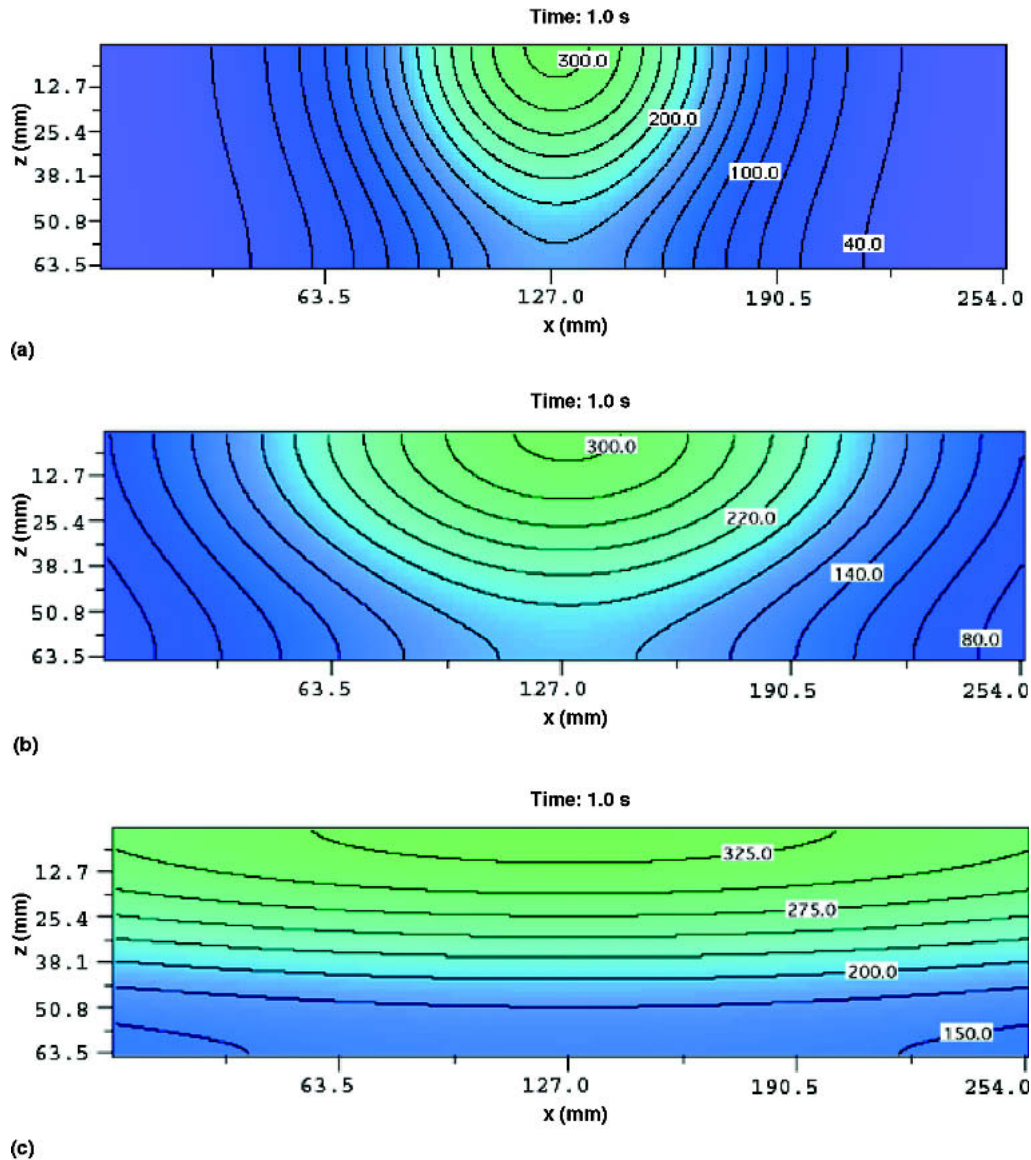


Fig. 6 Simulations of heat transfer within the prototype cable structure corresponding to the three different modes of heat conduction. Case (c) is characteristic of the actual physical response of the prototype C-fiber composite strand cable structure. Two-dimensional slice of the three-dimensional temperature field at 1 s

prototype analysis, the total time period of the experimental measurements, 500 s, is that which is assumed as the time prior to failure.

The inverse model defined by Eq 1 and 2 is a function of the adjustable parameters $C(x_k, y_k, z_k)$, κ_1 , κ_2 , κ_3 , and Δt . For the purpose of this prototype analysis, the authors consider only adjustment of the parameters $C(x_k, y_k, z_k)$ and κ_1 . This is consistent with the authors' use of two thermocouple measurements of temperature histories. The values of κ_2 , and κ_3 , are assigned according to their relationship to κ_1 . This relationship is specified according to the mode of heat conduction occurring within the wire structure. Three modes of heat conduction are considered: purely isotropic, moderately anisotropic, and anisotropic (typical of laminate wire structures). A typical value of κ_2/κ_1 for a graphite/epoxy laminate is 0.01757, which the

authors have adopted for their prototype analysis. The discrete time step Δt and the total number of time steps N_t were 0.4865 s and 1000, respectively.

Shown in Fig. 5 are the calculated temperature histories, at the locations of thermocouple measurement, corresponding to three different modes of heat conduction within the prototype cable structure. For each case, the values of $C(x_k, y_k, z_k)$ and κ_1 have been adjusted so as to achieve the best correspondence of the calculated and measured temperature histories over the entire time interval extending over 500 s. The spatial distribution of $C(x_k, y_k, z_k)$ was that of the decomposition pattern shown in Fig. 3 such that the discrete locations (x_k, y_k, z_k) were at a grid spacing $\Delta l = 1.27 \times 10^{-3}$ m. Shown in Fig. 6 to 9 are simulations of heat transfer within the prototype cable structure over a period of time prior to the assumed point of thermal break-

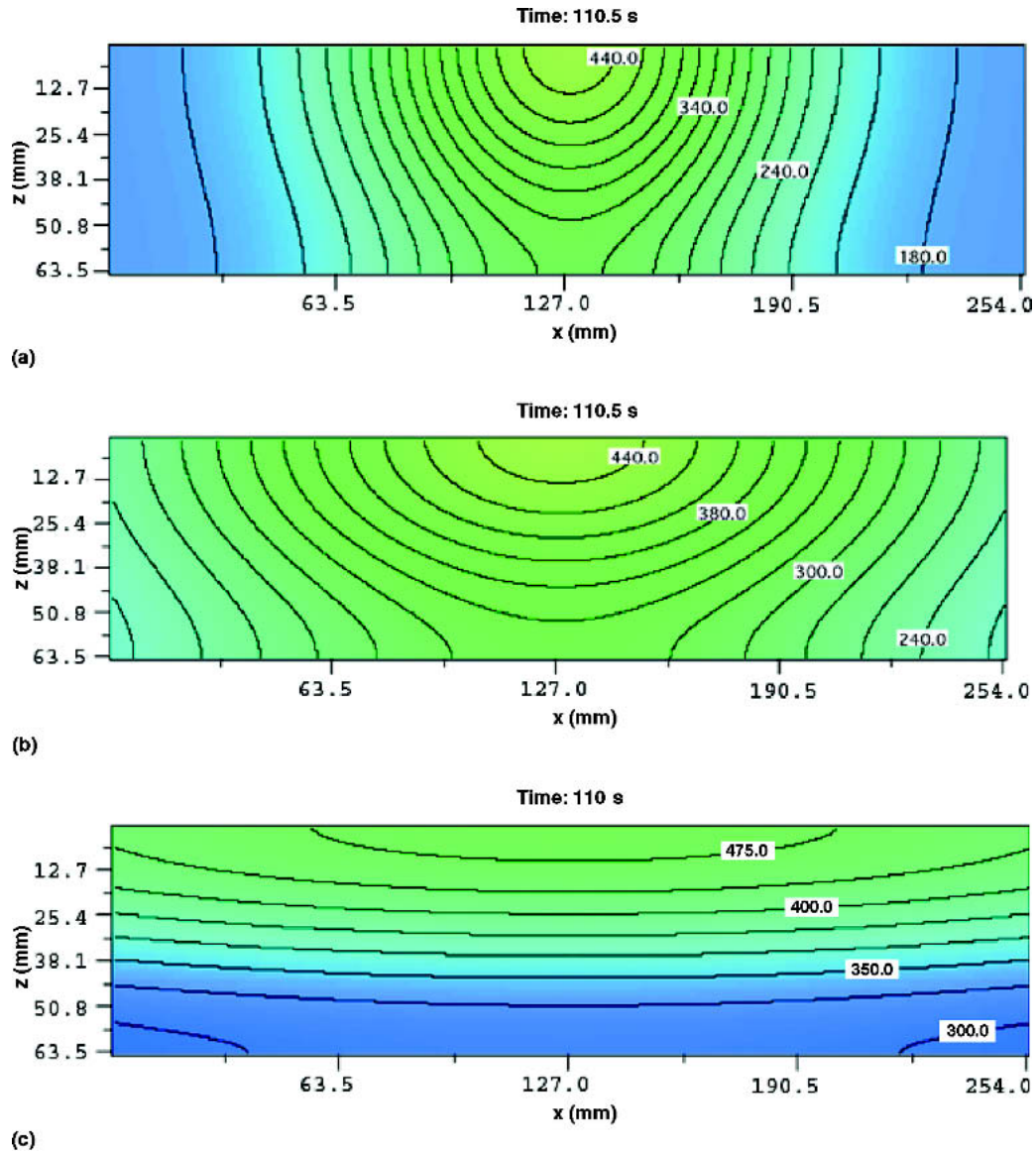


Fig 7 Simulations of heat transfer within the prototype cable structure corresponding to the three different modes of heat conduction. Case c is characteristic of the actual physical response of the prototype C-fiber composite strand cable structure. Two-dimensional slice of three-dimensional temperature field at 110 s

down corresponding to the three different modes of heat conduction: $\kappa_1 = 7.7 \times 10^{-4} \text{ m}^2/\text{s}$, $\kappa_2 = \kappa_1$, $\kappa_3 = \kappa_1$; $\kappa_1 = 3.0 \times 10^{-3} \text{ m}^2/\text{s}$, $\kappa_2 = 0.27 \kappa_1$, $\kappa_3 = \kappa_2$; and $\kappa_1 = 3.7 \times 10^{-3} \text{ m}^2/\text{s}$, $\kappa_2 = 0.0176\kappa_1$, $\kappa_3 = \kappa_2$. The time-dependent temperature fields shown in Fig. 6 to 9 are for the xz -plane at the midpoint of the y -axis (Fig. 1).

4. Discussion and Conclusions

The simulations shown in Fig. 6 to 8 are for a heat source having the characteristics of the experimental arrangement described by Fig. 2 and 3. The values of the parameters $C(x_k, y_k, z_k)$, κ_1 , κ_2 , κ_3 , and Δt have been adjusted according to the inverse model defined by Eq 1 and 2 with respect to this specific heat source. These parameters will, in principle, provide

an estimate of the response of the wire structure to heat sources having different spatial and temporal characteristics.

The level of anisotropy is specified according to the ratio κ_1/κ_2 (where $\kappa_3 = \kappa_2$). In practice, this quantity may be assigned according to the temperature history measured by an additional thermocouple measurement at a different location along the x -coordinate. One can, in principle, adjust both κ_1/κ_2 and κ_1/κ_3 according to the temperature histories measured by two additional thermocouples. In the case of more than three measured temperature histories, the model parameters should be optimized following a least-squares procedure (Ref 3).

The simulations presented in this study serve to isolate two properties of complex cable structures contributing to their ability to resist degradation due to external heating. One property, the average diffusivity κ_1 for heat transfer along the length

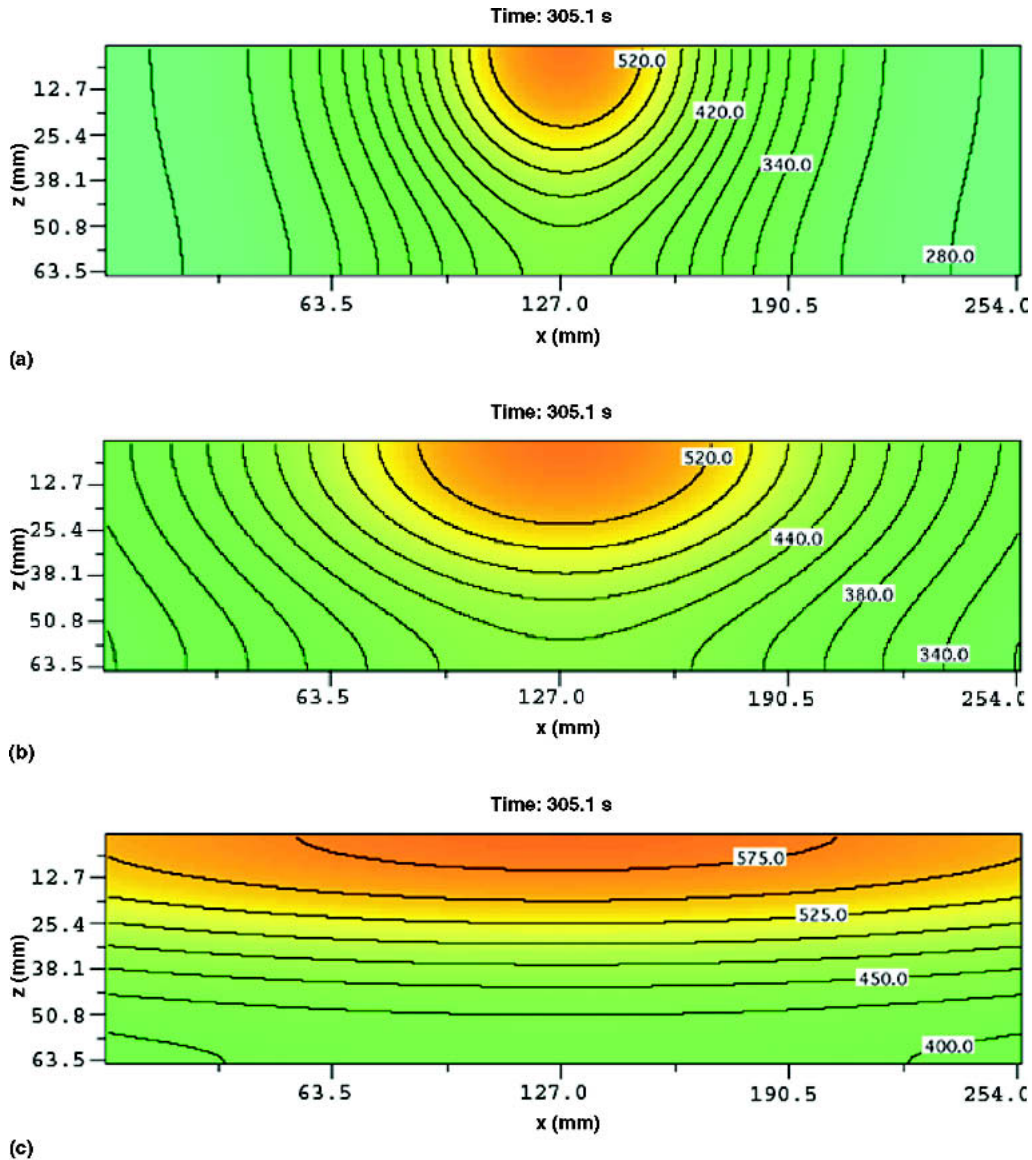


Fig. 8 Simulations of heat transfer within the prototype cable structure corresponding to the three different modes of heat conduction. Case c is characteristic of the actual physical response of the prototype C-fiber composite strand cable structure. Two-dimensional slice of three-dimensional temperature field at 305.1 s

of the cable structure, is representative of the capacity of the surface of the cable structure to resist heating. Relatively low values of κ_1 , which correlate with relatively high heat capacities of the materials, would imply a good barrier to heat transfer to locations within cable structures. The other property is the level of anisotropy within the transverse cross section of the cable structure, which was specified according to the ratios κ_1/κ_2 and κ_1/κ_3 . These ratios represent the capacity of the internal configuration of the cable structure to resist heat transfer along directions within the transverse cross section of the cable structure.

The significant feature of a method, based on inverse analysis, is its convenient applicability for analysis of the performance of multifunctional cable structures subject to external heating. Although this method employs a parametric model

representation defined in terms of a rectangular cross section, it is sufficiently general for the representation of anisotropic heat transfer within a cable structure of arbitrary cross section. Consistent with the inverse-modeling approach, the model parameters are assumed to represent the average or “lumped” response of a complex cable structure, the cross section of which is characterized by a heterogeneous distribution of different types of materials. It follows, therefore, that values of the model parameters, obtained by “inversion” of thermocouple measurements, are not sensitive to details concerning the cross sectional shape of a given cable structure. This insensitivity, based on the assumed nature of the model parameters, provides a basis for representing heat transfer in complex cable structures by the relatively simple and convenient model defined by Eq 1 and 2.

Finally, it is important to note that the model presented here considers only one aspect of the overall process of thermal degradation within multicomponent tensioned cable structures. A complete characterization of such degradation by means of a model must consider the physical nature of the coupling between the impinging hot-gas plume and the surface of the cable structure, as well as the coupling between the heat transfer and mechanical response properties of the cable structure. In principle, the temperature fields calculated by means of the inverse model defined by Eq 1 and 2 should be easily combined with model representations of these other aspects of thermal degradation within cable structures. The goal for the development of such model representations, however, should still be a minimization of the inclusion of inconvenient levels of complexity. This goal is usually achieved using methods based on inverse analysis. The advantage of using inverse models to calculate temperature histories within complex cable structures is that

they provide a basis for predicting failure rates under different types of heating conditions.

Acknowledgments

Support for this work was provided by the Office of Naval Research.

References

1. K.A. Woodbury, Ed., *Inverse Engineering Handbook*, CRC Press, 2003
2. S.G. Lambrakos, R.W. Fonda, J.O. Milewski, and J.E. Mitchell, *Sci. Technol. Weld. Join.*, Vol 8, 2003, p 345
3. M. Rappaz, M. Bellet, and M. Deville, *Numerical Modeling in Materials Science and Engineering*, Springer-Verlag, Berlin, 2003, p 448-475
4. H.S. Carslaw and J.C. Jaeger, *Conduction of Heat in Solids*, 2nd ed., Clarendon Press, Oxford, 1959, p 374